Recombination and localization

Unfolding the pathways behind conductivity losses in $Cs_2AgBiBr_6$ thin films

Jöbsis, Huygen J.; Caselli, Valentina M.; Askes, Sven H.C.; Garnett, Erik C.; Savenije, Tom J.; Rabouw, Freddy T.; Hutter, Eline M.

DOI
10.1063/5.0061899

Publication date
2021

Document Version
Final published version

Published in
Applied Physics Letters

Applied Physics Letters

Recombination and localization: Unfolding the pathways behind conductivity losses in $Cs_2AgBiBr_6$ thin films

Cite as: Appl. Phys. Lett. **119**, 131908 (2021); https://doi.org/10.1063/5.0061899
Submitted: 30 June 2021 • Accepted: 11 September 2021 • Published Online: 30 September 2021

Huygen J. Jöbsis, Valentina M. Caselli, Sven H. C. Askes, et al.

COLLECTIONS

Paper published as part of the special topic on New Solution-processed Perovskites and Perovskite-inspired Optoelectronic Materials and Devices

This paper was selected as an Editor's Pick

Applied Physics Letters ARTICLE scitation.org/journal/apl

Recombination and localization: Unfolding the pathways behind conductivity losses in $Cs_2AgBiBr_6$ thin films

Cite as: Appl. Phys. Lett. **119**, 131908 (2021); doi: 10.1063/5.0061899
Submitted: 30 June 2021 · Accepted: 11 September 2021 ·
Published Online: 30 September 2021

View Online Export Citation CrossMark

Huygen J. Jöbsis,[1] Valentina M. Caselli,[2] Sven H. C. Askes,[3] Erik C. Garnett,[3] Tom J. Savenije,[2] Freddy T. Rabouw,[1,a)] and Eline M. Hutter[1,a)]

AFFILIATIONS

[1]Inorganic Chemistry and Catalysis, Department of Chemistry, Utrecht University, Princetonlaan 8, 3584 CB Utrecht, The Netherlands
[2]Department of Chemical Engineering, Delft University of Technology, van der Maasweg 9, 2629 HZ Delft, The Netherlands
[3]Center for Nanophotonics, AMOLF, 1098 XG Amsterdam, The Netherlands

Note: This paper is part of the APL Special Collection on New Solution-processed Perovskites and Perovskite-inspired Optoelectronic Materials and Devices.
[a)]**Authors to whom correspondence should be addressed:** f.t.rabouw@uu.nl and e.m.hutter@uu.nl

ABSTRACT

$Cs_2AgBiBr_6$ (CABB) has been proposed as a promising nontoxic alternative to lead halide perovskites. However, low charge carrier collection efficiencies remain an obstacle for the incorporation of this material in optoelectronic applications. In this work, we study the optoelectronic properties of CABB thin films using steady state and transient absorption and reflectance spectroscopy. We find that optical measurements on such thin films are distorted as a consequence of multiple reflections within the film. Moreover, we discuss the pathways behind conductivity loss in these thin films, using a combination of microsecond transient absorption spectroscopy and time-resolved microwave conductivity measurements. We demonstrate that a combined effect of carrier loss and localization results in the conductivity loss in CABB thin films. Moreover, we find that the charge carrier diffusion length and grain size are of the same order of magnitude. This suggests that the material's surface is an important contributor to charge-carrier loss.

Lead-halide perovskites exhibit excellent light absorption and emission properties and micrometer-long charge carrier diffusion length, making them interesting for optoelectronic applications.[1,2] However, the presence of lead and iodide ions raises toxicity concerns.[3,4] In addition, many of the lead-based perovskites have poor stability in the aqueous environment, limiting their application in, e.g., photocatalysis.[5] Cesium silver bismuth bromide ($Cs_2AgBiBr_6$, CABB) has been suggested as a less toxic and more stable alternative for the remarkably performing lead-halide perovskites in optoelectronic applications.[6–10]

Microsecond-long carrier lifetimes, increased stability in water, and improved photostability with respect to high performing lead-containing analogues have triggered an extensive research effort into CABB.[8,9,11–14] Its applicability in solar conversion or lighting applications is still limited due to the weak absorption and emission caused by the indirect bandgap.[15,16] On the other hand, the material performs well as an x-ray detector.[17,18] This can be understood from the presence of bismuth, causing efficient x-ray attenuation and the long carrier lifetimes, which are desirable for charge extraction. More recently, CABB was also used for photocatalytic reactions such as light-driven CO_2 conversion and H_2 generation from hydrobromic acid.[5,19] However, in all of these applications, the charge extraction efficiency remains limited by the short diffusion length of the minority carrier. The limited extraction has been ascribed to the high trap density in CABB single crystals compared to lead-containing perovskite single crystals.[20] In a recent study, Wright *et al.* identified charge carrier self-localization to a small polaronic state with a localization rate of ca. 1 ps^{-1} to be intrinsic to CABB.[21] Such fast localization rates would be detrimental to its application in optoelectronic devices. However, temperature-activated delocalization results in appreciable carrier mobilities at room temperature.[20,21] Moreover, mobile carriers were observed for microseconds after photoexcitation at elevated

temperatures,[20] highlighting CABB as a potential alternative for lead-halide analogs.

In this work, we study the charge-carrier dynamics in CABB thin films on nanosecond-to-microsecond timescales using a combination of transient absorption (TA) spectroscopy and time-resolved microwave conductivity measurements. TA experiments present long-lived carriers ranging over several microseconds, while TRMC measurements on the same thin films show that all charge carriers are immobilized within 200 ns. In the first tens of nanoseconds, the charge carrier mobility remains almost constant, indicating that the intensity drop of the TRMC trace on this timescale is the result of carrier loss, after which it drops due to localization of remaining carriers. So that we conclude that the conductivity loss in CABB thin films is the result of both carrier loss and localization. A comparison of the bleach recovery dynamics of the direct and indirect absorptions shows that photogenerated electrons are lost more rapidly than holes. Carrier diffusion lengths of the same order of magnitude as the film thickness and the crystal grain size suggest a dominant role of the material's surface and grain boundaries in charge-carrier loss.

We prepared CABB thin films of ca. 100 nm thick, following the method by Li *et al.*[22] In short, a mixture of CsBr, AgBr, and $BiBr_3$ in dimethyl sulfoxide was spin coated on an optical substrate, allowed to dry, and annealed. The corresponding x-ray diffraction (XRD) pattern confirms the cubic phase group $Fm\bar{3}m$ (Fig. S1).[8] Atomic force microscopy shows a homogeneous film coverage with a root mean square roughness of 7.3 nm (Fig. S2). Scanning electron microscopy shows an average grain size of ca. 100 nm (Fig. S3). Further experimental details are provided in the supplementary material.

The steady-state optical properties were determined using an UV-vis spectrometer with an integrating sphere (see experimental methods). The transmittance (T) spectrum, i.e., the fraction of light transmitted as a function of the photon energy, shows a characteristic dip around 2.8 eV [blue line in Fig. 1(a)]. This energy is significantly larger than the energy of the bandgap of CABB, which is indirect and, therefore, does not cause a distinct dip in the transmittance spectrum. The feature at 2.8 eV is instead often attributed to the excitonic transition between conduction and valence bands at the Γ point in the dispersion diagram [Fig. 1(b)].[23] We attribute the slow decrease in the transmittance, starting at 2.2 eV and increasing toward higher energies, to indirect absorption. Indeed, the indirect-bandgap energy of CABB single crystals,[11,24] thin films,[8,9] and nanocrystals[25,26] is reported ranging from 1.95 to 2.3 eV. The photoluminescence (PL) [black line, Fig. 1(a)] is considerably red-shifted compared to the indirect-bandgap absorption and relatively broad (centered at 1.9 eV, FWHM of 515 meV). The red-shift is known to be due to strong exciton phonon coupling.[8,11,21,27] Recent work suggests that the charge carrier recombination pathway in CABB proceeds via color centers.[21,24]

We observe oscillations in the reflectance (R, the fraction of light reflected) spectrum [green line in Fig. 1(a)]. These must be due to a combination of absorption resonances of CABB and the film's dielectric properties, which determine interference effects. The real part of a material's dielectric function peaks at frequencies just below an absorption resonance, while it shows a minimum at frequencies just above the resonance. As the reflectance of a bulk material scales with the dielectric contrast with air, it should peak just below a strong absorption resonance and dip at energies above the resonance. Indeed, R of our CABB film shows such a wiggle feature around the excitonic resonance at 2.8 eV [Fig. 1(a)]. A similar feature is not obvious around the indirect bandgap transition at 2.2 eV, which is likely the result of interference between multiple reflections within the film distorting the reflectance spectrum. Interference becomes an especially important factor determining the film's reflectivity in the spectral range below 2.8 eV, where the absorption of CABB is weak compared to the film thickness of 100 nm [Fig. 1(c); calculated based on ellipsometry data Fig. S4] so multiple reflections of the light are possible.

Next, we study the change in optical properties using pump-probe TA spectroscopy experiments in the transmission mode on a microsecond timescale (for a schematic of the TA setup, see Fig. S5 in the supplementary material).[28] The transient transmittance ($\Delta T/T$) shows a distinct bleach at 2.8 eV, which is present for excitation at energies above as well as below the direct transition [compare blue and green lines in Fig. 2(a)]. The bleach must, therefore, be due to holes near the top of the valence band, which can be photoexcited with either direct or indirect excitation. For excitation at 355 nm (3.5 eV), an additional weak and broad bleach feature between 1.8 and 2.2 eV is present. This energy range comprises the reported values for the indirect bandgap of CABB. We propose that this signal is the result of a combination of absorption and reflection effects, which we will discuss below. The broad bleach signal is not as evident for excitation at 532 nm (2.3 eV) because of the low signal to noise ratio.

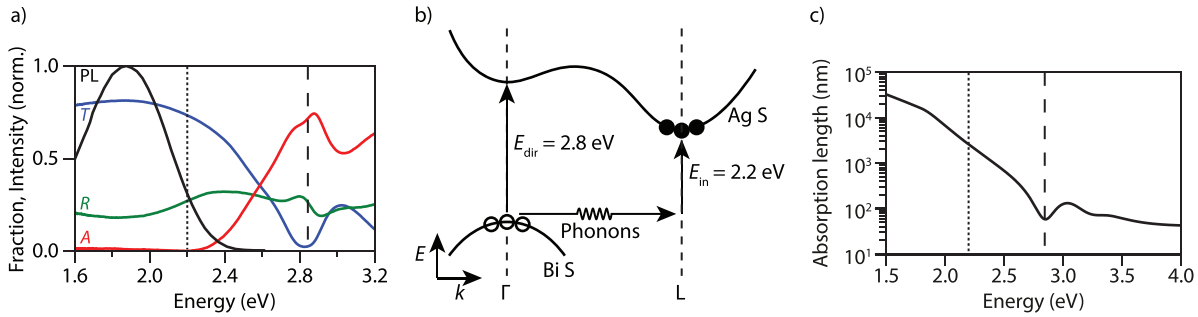

FIG. 1. Optical properties of CABB thin films. (a) The fraction of transmitted (T, blue line), reflected (R, green line), and absorbed (A, red line) light, as well as the photoluminescence intensity (PL, black line, $\lambda_{exc} = 440$ nm) as a function of the photon energy for a 100-nm-thick CABB film on glass. (b) Schematic representation of the band structure of CABB, showing the direct and indirect absorption processes. (c) The absorption length as a function of the photon energy calculated based on ellipsometry data. The dotted and dashed lines in panels (a) and (c) represent the indirect bandgap and excitonic transition in CABB.

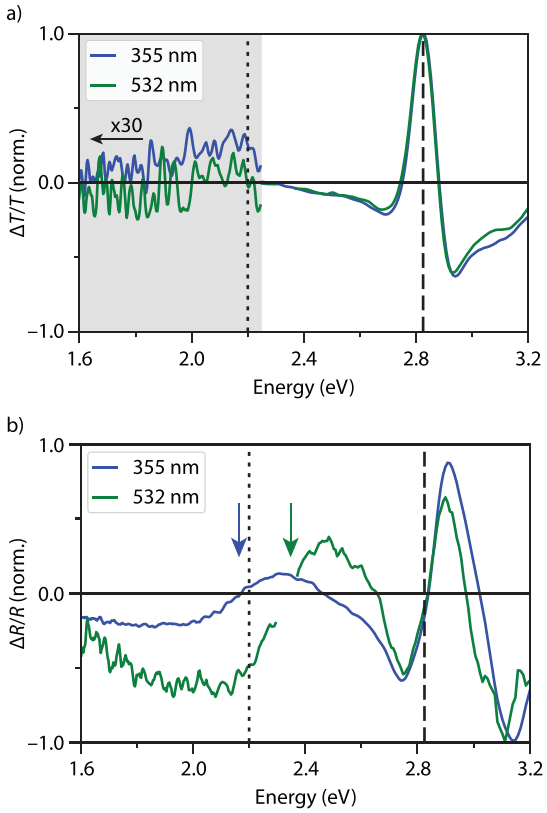

FIG. 2. Transient transmittance and reflectance spectral slices. (a) Normalized spectral slice of $\Delta T/T$ for excitation at 355 (blue) and 532 nm (green) after a delay time of 100 ns. In the grey-shaded area, the data are magnified by a factor of 30. (b) Normalized spectral slice of $\Delta R/R$ for excitation at 355 nm (blue) and 532 nm (green) after a delay time of 100 ns. The blue and green arrows indicate the inflection point of $\Delta R/R$ for excitation at 355 and 532 nm, respectively. In both panels, the dotted and dashed lines, respectively, represent the indirect bandgap and excitonic transition of CABB.

In the reflection mode, we study the change in reflectance of our CABB thin films, again for excitation at 355 and 532 nm [Fig. 2(b)]. The $\Delta R/R$ spectrum displays much stronger features in the indirect-absorption region (<2.7 eV) than the $\Delta T/T$ spectrum, highlighting the potential to extract information on indirect-absorption transitions from reflectivity measurements. However, the interpretation of the spectra is not straightforward. For both excitation wavelengths, we observe an inflection point in $\Delta R/R$ at 2.8 eV: decreased reflectance just below and increased reflectance just above the absorption resonance. This results in a minimum in $\Delta R/R$ at 2.75 eV followed by a maximum at 2.9 eV. This spectral shape is a consequence of the bleach of the absorption transition. Bleaching the absorption flattens the real part of the material's dielectric function around the absorption resonance and suppresses the wiggle in the reflectivity spectrum (see discussion above). For both excitation wavelengths, a second inflection point is observed at lower energies. For excitation at 355 nm the inflection point occurs at 2.2 eV, while it is at 2.4 eV for 532-nm excitation [compare blue and green arrows in Fig. 2(b)]. While these are the approximate energies of the indirect bandgap in CABB, the different inflection points for different excitation wavelengths indicate that inflections are not just due to a bleach of the indirect absorption. Instead, the $\Delta R/R$ spectrum at <2.7 eV is likely strongly distorted by interference effects in the thin film. Indeed, our CABB film is 100 nm thick and has a refractive index of approximately 2, so the light of 1.6 eV picks up a phase of π upon back-and-forth reflection in the film, which increases to 1.7π at 2.7 eV, causing a slow variation of the interference over this range of photon energies. Considering the absorption length at the excitation wavelength [Fig. 1(c)], the 355-nm excitation will generate charge carriers mostly at the surface, while 532-nm excitation generates charge carriers more homogeneously. It is unclear to what extent this affects interference of probe light within the film. It is, therefore, not straightforward to assign the spectral features in the $\Delta R/R$ spectrum at <2.7 eV to any particular transition. We note that interference also affects a film's differential transmission ΔT (or its differential absorptance or differential absorbance) whenever the absorption length [Fig. 1(c)] is long compared to the film thickness, so care must be taken in the interpretation of spectra. Figs. S6 and S7 in the supplementary material present the $\Delta T/T$ and $\Delta R/R$ spectra of our films as a function of delay time.

Finally, we study the charge carrier decay dynamics for our CABB thin films. The $\Delta T/T$ traces for both bleach signals [direct transition at 2.82 eV (blue) and indirect transition at 2.2 eV (red)] are shown for excitation at 355 nm in Fig. 3(a). We observe a long-lived tail ranging over several microseconds in both measurements. Such slow decay dynamics in TA experiments on CABB thin films have previously been observed in the literature.[11,29] In contrast, TRMC measurements [black in Fig. 3(a)] on the same CABB thin films show that 99% of free-carrier mobility is lost within 200 ns after photoexcitation. These observations indicate that although the photoexcited electrons and holes localize on timescales of tens of nanoseconds (losing mobility), recombination extends over several microseconds. The bleach of the indirect absorption drops considerably faster in the first 100 ns than that of the direct absorption. Typically, on this timescale, the charge carriers have relaxed to the band edges so that the charge carriers occupy their corresponding bands as depicted in Fig. 1(b). From this, it follows that the bleach recovery dynamics of the indirect transition scale with both the electron and hole population, whereas the direct-absorption bleach depends only on the hole population. We have to note that the TA and TRMC experiments discussed in this work do not provide insight on sub-nanosecond kinetics (see the supplementary material for more experimental details). The decay dynamics do not depend significantly on the excitation wavelength (Fig. S8).

As opposed to Pb-based perovskites, which show strong fluence-dependent lifetimes due to higher order recombination,[3] the lifetimes of CABB barely change with fluence (Fig. S9). This allows comparison between the TA and TRMC traces in spite of slightly different excitation densities. The TRMC signal probes the product of charge carrier concentration and mobility, whereas the TA signal scales only with the concentration. Assuming that all charge carriers contribute equally to the TA signal, independent of the degree of localization, the ratio between the TRMC and TA traces reveals the decay of overall mobility of photoexcited charge carriers. As discussed above, the TA trace observed for the indirect transition scales with both the electron and hole population, so that comparison of this trace with the TRMC traces provides insight into the mobility over time. For delay times

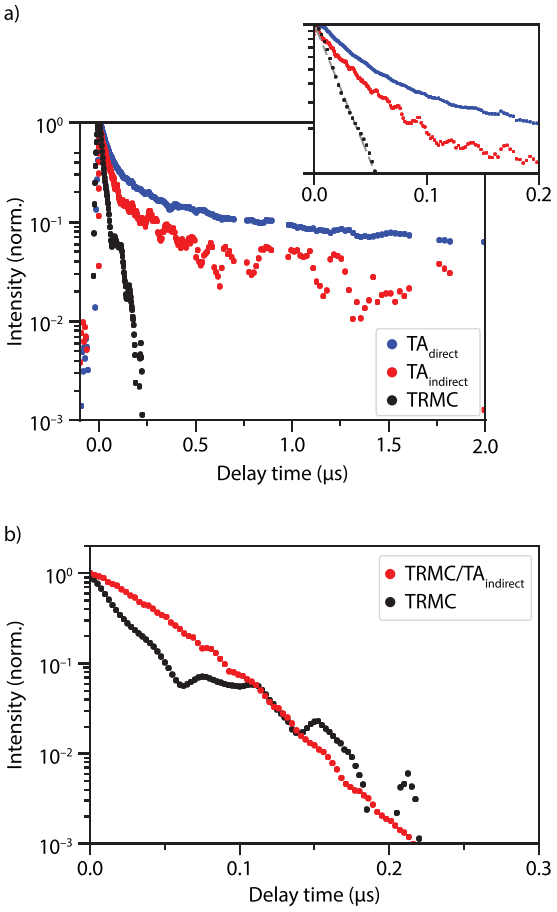

FIG. 3. TA and TRMC time traces. (a) Normalized TA time traces at 2.2 (red) and 2.8 eV (blue) ($\lambda_{exc} = 355$ nm). Normalized TRMC time trace (black, $\lambda_{exc} = 355$ nm). The inset is a zoom-in of the kinetics between 0 and 200 ns. A single exponential function was fit to the TRMC data (grey dashed line). (b) The calculated mobility trace (red) by taking the ratio between the TRMC fit and the TA trace observed for the indirect transition. For clarity, the TRMC trace in panel (a) is reproduced in black. All traces are normalized to unity at $t = 0$.

<40 ns, the TRMC and TA traces observed for the indirect transition show similar decay kinetics [the inset of Fig. 3(a)]. This means that the mobility remains close to constant and, on this timescale, both carriers are mobile and the conductivity loss is the result of charge carrier loss. Interestingly, we observe a short-lived plateau in the bleach recovery dynamics of the direct transition (depending only on hole population), indicating that in the first 10 ns after photoexcitation, the hole population remains close to constant. This suggests that the initial drop in the TRMC signal over the first 10 ns is the result of a change in the electron population density. On the timescales from 10 to 40 ns, both electrons and holes are lost, and the mobility of remaining carriers is unaffected [Fig. 3(b)]. Beyond 40 ns, the charge carriers localize, and their mobility goes down. More experiments would be necessary to distinguish how much electrons and holes contribute to the overall conductivity.

With the use of the carrier mobility and the free-carrier half lifetime, i.e., the time after which the TRMC signal has decayed by a factor two, we can estimate the carrier diffusion length.[30] The maximum signal height of the TRMC trace represents the yield-mobility product, $\varphi \sum \mu = 0.11\ \mathrm{cm^2\ V^{-1}\ s^{-1}}$ [Fig. S9(d)], where the summation runs over the contributions of electrons and holes.[31] This is lower than the range of mobilities reported in the literature,[32] and this can be understood considering that $\varphi < 1$. Using this value and a free-carrier half lifetime of 35 ns, we estimate the charge carrier diffusion length to be 100 nm (Table S1). This is the same length scale as the thickness of our film and the crystal grain size of the material. In the literature, it has been suggested that surface-related charge carrier recombination limits the photoconductance in CABB thin films.[20] Based on our observation discussed above, we can similarly conclude that the decay in photoconductivity is likely the result of trapping at the film surface and/or grain boundaries. This would mean that the photoconductance can be increased through, e.g., surface passivation, further improving the potential of CABB-based optoelectronic applications.

In this work, we studied the steady-state and transient optical properties of CABB thin films. The steady-state transmission spectrum on the thin films clearly shows the direct absorption transition at 2.8 eV. The indirect bandgap is, however, not distinctly present. The reflectance R and transient reflectance $\Delta R/R$ spectra show features in the indirect-bandgap region. They are likely dominated by multiple interference effects in the thin CABB film and difficult to assign to any particular electronic transition. Further research into the influence of such interference effects on R and $\Delta R/R$ is required, including possible influences of a nonhomogeneous charge carrier distribution, as this will ultimately affect the absorption for thin films in spectroscopic studies as well as applications.

TA spectroscopy revealed that the charge carrier density decays on a 40-ns timescale, but a fraction of the photogenerated holes near the valence band maximum have a lifetime ranging over several microseconds. TRMC measurements showed that these long-lived carriers are, however, not mobile. Comparison of the TRMC and TA traces shows that the conductivity loss is the result of a combined effect of charge carrier loss and localization. Finally, we find that the charge carrier diffusion length is of the same order of magnitude as the film thickness and the grain size, suggesting that trapping at the film surface or at grain boundaries leads to a decay in photoconductivity. This means that the photoconductance can be increased through improved material design, further enhancing the potential of CABB for optoelectronic applications. Follow-up work could test this hypothesis by systematically studying films of varying thicknesses.

See the supplementary material for details on the synthesis and the experimental methods.

H.J.J. and E.M.H. acknowledge funding from the Dutch Research Council (NWO) under Grant No. VI.Veni.192.034. H.J.J. and E.M.H. are further supported by the Advanced Research Center Chemical Building Blocks Consortium (ARC CBBC). V.M.C. and T.J.S. acknowledge funding from the Dutch Research Council (NWO), Grant No. 739.017.004. S.H.C.A. acknowledges funding from the Dutch Research Council (NWO), Grant No. VI.Veni.192.062.

DATA AVAILABILITY

The data that support the findings of this study are available from the corresponding authors upon request.

REFERENCES

[1]S. D. Stranks and H. J. Snaith, Nat. Nanotechnol. **10**, 391 (2015).
[2]M. B. Johnston and L. M. Herz, Acc. Chem. Res. **49**, 146 (2016).
[3]E. M. Hutter, R. Sangster, C. Testerink, B. Ehrler, and C. M. M. Gommers, arXiv:2012.06219 (2020).
[4]A. Babayigit, A. Ethirajan, M. Muller, and B. Conings, Nat. Mater. **15**, 247 (2016).
[5]H. Huang, B. Pradhan, J. Hofkens, M. B. J. Roeffaers, and J. A. Steele, ACS Energy Lett. **5**, 1107 (2020).
[6]T. Jafari, E. Moharreri, A. Amin, R. Miao, W. Song, and S. Suib, Molecules **21**, 900 (2016).
[7]A. H. Slavney, R. W. Smaha, I. C. Smith, A. Jaffe, D. Umeyama, and H. I. Karunadasa, Inorg. Chem. **56**, 46 (2017).
[8]A. H. Slavney, T. Hu, A. M. Lindenberg, and H. I. Karunadasa, J. Am. Chem. Soc. **138**, 2138 (2016).
[9]E. T. McClure, M. R. Ball, W. Windl, and P. M. Woodward, Chem. Mater. **28**, 1348 (2016).
[10]Z. Xiao, Z. Song, and Y. Yan, Adv. Mater. **31**, 1803792 (2019).
[11]R. L. Z. Hoye, L. Eyre, F. Wei, F. Brivio, A. Sadhanala, S. Sun, W. Li, K. H. L. Zhang, J. L. MacManus-Driscoll, P. D. Bristowe, R. H. Friend, A. K. Cheetham, and F. Deschler, Adv. Mater. Interfaces **5**, 1800464 (2018).
[12]E. Greul, M. L. Petrus, A. Binek, P. Docampo, and T. Bein, J. Mater. Chem. A **5**, 19972 (2017).
[13]G. Volonakis, M. R. Filip, A. A. Haghighirad, N. Sakai, B. Wenger, H. J. Snaith, and F. Giustino, J. Phys. Chem. Lett. **7**, 1254 (2016).
[14]L. Schade, A. D. Wright, R. D. Johnson, M. Dollmann, B. Wenger, P. K. Nayak, D. Prabhakaran, L. M. Herz, R. Nicholas, H. J. Snaith, and P. G. Radaelli, ACS Energy Lett. **4**, 299 (2019).
[15]C. N. Savory, A. Walsh, and D. O. Scanlon, ACS Energy Lett. **1**, 949 (2016).
[16]G. Longo, S. Mahesh, L. R. V. Buizza, A. D. Wright, A. J. Ramadan, M. Abdi-Jalebi, P. K. Nayak, L. M. Herz, and H. J. Snaith, ACS Energy Lett. **5**, 2200 (2020).
[17]W. Pan, H. Wu, J. Luo, Z. Deng, C. Ge, C. Chen, X. Jiang, W.-J. Yin, G. Niu, L. Zhu, L. Yin, Y. Zhou, Q. Xie, X. Ke, M. Sui, and J. Tang, Nat. Photonics **11**, 726 (2017).
[18]Z. Zhang, C. C. Chung, Z. Huang, E. Vetter, D. Seyitliyev, D. Sun, K. Gundogdu, F. N. Castellano, E. O. Danilov, and G. Yang, Mater. Lett. **269**, 127667 (2020).
[19]L. Zhou, Y.-F. Xu, B.-X. Chen, D.-B. Kuang, and C.-Y. Su, Small **14**, 1703762 (2018).
[20]D. Bartesaghi, A. H. Slavney, M. C. Gélvez-Rueda, B. A. Connor, F. C. Grozema, H. I. Karunadasa, and T. J. Savenije, J. Phys. Chem. C **122**, 4809 (2018).
[21]A. D. Wright, L. R. V. Buizza, K. J. Savill, G. Longo, H. J. Snaith, M. B. Johnston, and L. M. Herz, J. Phys. Chem. Lett. **12**, 3352 (2021).
[22]Z. Li, S. R. Kavanagh, M. Napari, R. G. Palgrave, M. Abdi-Jalebi, Z. Andaji-Garmaroudi, D. W. Davies, M. Laitinen, J. Julin, M. A. Isaacs, R. H. Friend, D. O. Scanlon, A. Walsh, and R. L. Z. Hoye, J. Mater. Chem. A **8**, 21780 (2020).
[23]B. A. Connor, L. Leppert, M. D. Smith, J. B. Neaton, and H. I. Karunadasa, J. Am. Chem. Soc. **140**, 5235 (2018).
[24]S. J. Zelewski, J. M. Urban, A. Surrente, D. K. Maude, A. Kuc, L. Schade, R. D. Johnson, M. Dollmann, P. K. Nayak, H. J. Snaith, P. Radaelli, R. Kudrawiec, R. J. Nicholas, P. Plochocka, and M. Baranowski, J. Mater. Chem. C **7**, 8350 (2019).
[25]S. E. Creutz, E. N. Crites, M. C. De Siena, and D. R. Gamelin, Nano Lett. **18**, 1118 (2018).
[26]B. Yang, J. Chen, S. Yang, F. Hong, L. Sun, P. Han, T. Pullerits, W. Deng, and K. Han, Angew. Chem. Int. Ed. **57**, 5359 (2018).
[27]J. A. Steele, P. Puech, M. Keshavarz, R. Yang, S. Banerjee, E. Debroye, C. W. Kim, H. Yuan, N. H. Heo, J. Vanacken, A. Walsh, J. Hofkens, and M. B. J. Roeffaers, ACS Nano **12**, 8081 (2018).
[28]S. O. M. Hinterding, B. B. V. Salzmann, S. J. W. Vonk, D. Vanmaekelbergh, B. M. Weckhuysen, E. M. Hutter, and F. T. Rabouw, ACS Nano **15**, 7216 (2021).
[29]R. Kentsch, M. Scholz, J. Horn, D. Schlettwein, K. Oum, and T. Lenzer, J. Phys. Chem. C **122**, 25940 (2018).
[30]E. M. Hutter, M. C. Gélvez-Rueda, D. Bartesaghi, F. C. Grozema, and T. J. Savenije, ACS Omega **3**, 11655 (2018).
[31]T. J. Savenije, A. J. Ferguson, N. Kopidakis, and G. Rumbles, J. Phys. Chem. C **117**, 24085 (2013).
[32]J. Leveillee, G. Volonakis, and F. Giustino, J. Phys. Chem. Lett. **12**, 4474 (2021).